DEVELOPMENT OF ENHANCED MOLD FLOW CONTROL IN SLAB CASTING

Martin Sedén[1], Jan-Erik Eriksson[1], Arnoud Kamperman[2], Edward Dekker[2], Johan Pejnefors[3] and Krister Fröjdh[3]

[1]ABB AB, Terminalvägen 24, SE-721 59 Västerås, Sweden
[2]Tata Steel Europe, P.O. Box 10000, 1970CA IJmuiden, Netherlands
[3]Proximion AB, Skalholtsgatan 10, SE-164 40 Kista, Sweden

Abstract

In view of its recognized potential in improving cast quality of slabs, the interest for electromagnetic devices has steadily increased over the years. Combining FC Mold for stirring and/or braking in the mold with a novel temperature measuring system, active control of the steel flow conditions close to the meniscus becomes within reach, enabling a vast improvement of surface and subsurface quality of the slab. In a collaboration between ABB, Proximion and Tata Steel Europe (IJmuiden), a single broad face copper plate has been equipped with a temperature measurement system based on optical FBG technology, having a staggering 2660 temperature measuring points. In the first eight months of operation, more than 2000 heats were cast using the mold equipped with this OptiMold System.

This paper reveals measured thermal results with an unprecedented temperature resolution in the mold plate, from which local casting phenomena in melt flow, shell and mold powder are illuminated. Some operational results and their correlation with meniscus conditions such as meniscus shape, flow symmetry and mold temperature are highlighted. Additionally, the process of how to control mold flow symmetry, meniscus flow speeds and process stability by an on-line closed-loop control system is presented.

Introduction

Electromagnetic flow control is a well-proven technology for quality improvements in continuous slab casting [1]-[4]. Inductive stirrers working based on travelling magnetic field principles have been proven particularly efficient for flow acceleration, temperature homogenization and inclusion washing in surface/subsurface regions of the strand. Different configurations of static magnetic fields have also been utilized to brake and stabilize high speed processes. For varying casting conditions such as throughput, slab format, slag type, steel grade, Argon flow injection, SEN type and immersion depth, mold level, etc., different electromagnetic settings need to be applied to create the best possible flow conditions. The appropriate settings can be found by trials and an experience database can slowly be built up. Another option to obtain good settings is to numerically simulate the process with modern computer technology and software. The drawback of both these methods is that they are time-consuming. A driver behind the OptiMold System is to measure flow conditions on-line and in real time adjust flow control device parameters accordingly. Another benefit of the same system is superior thermal monitoring resolution. The setup of the OptiMold Monitor, co-developed by ABB and Proximion and installed at Tata Steel Europe (IJmuiden), and its potential for enhanced mold flow control are presented in this paper.

Measurement System and Test Setup

The core of the installed OptiMold Monitor (Figure 1) is a set of 38 measuring optical fibers. One end is mounted into evenly spaced vertical holes in the top half of a new copper broad face plate, 15 mm from the hot face, and the other end is spliced to a multi-strand harsh environment collector cable in a connection box mounted on the side of the mold plate. At the mold end of each fiber, 70 Fiber Bragg Gratings (FBGs) have been accurately positioned every 5 mm [5], starting 30 mm from the top of the copper plate and covering the upper broad face down to 375 mm from top of copper. Each FBG acts as a single temperature sensor, thus in total equipping the broad face plate with 2660 sensors. See [10] for system setup details.
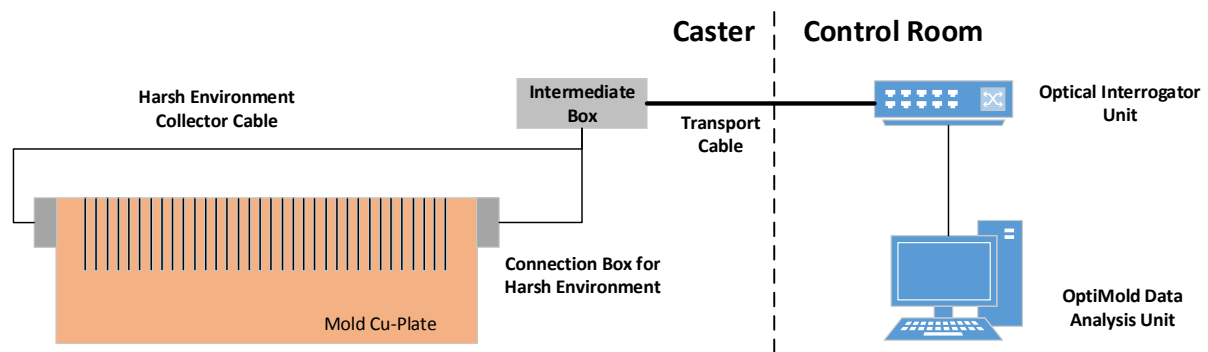

Figure 1. Schematic setup of OptiMold Monitor.

Four 15 m long collector cables are, through robust expanded beam connectors, plugged in to an intermediate box positioned close to the caster. From the intermediate box, the optical transmission is carried by a 125 m transport cable connecting all the caster fibers to interrogators in a climate controlled room. The light source in the interrogator sends a broadband light pulse into the fibers, and reflections caused by the FBGs are picked up by the interrogator unit and are translated by software to temperature data for all sensor points. Temperature data is scanned and treated on-line for the entire mold plate twice every second.

High Resolution Measurements of Heat Curves in Mold

Varying FC Mold Magnetic Field Levels

The slab caster at Tata Steel Europe (IJmuiden), where the OptiMold Monitor has been installed, is also equipped with an ABB FC Mold, a two-level electromagnetic brake to control the flow of the molten steel in the mold. During a trial campaign, the magnetic fields of the FC Mold were varied, as the OptiMold Monitor scanned the thermal status of the mold.

a.   1.0 m/min, 1100 mm, SENID = 190 mm   b.   1.9 m/min, 1100 mm, SENID = 190 mm
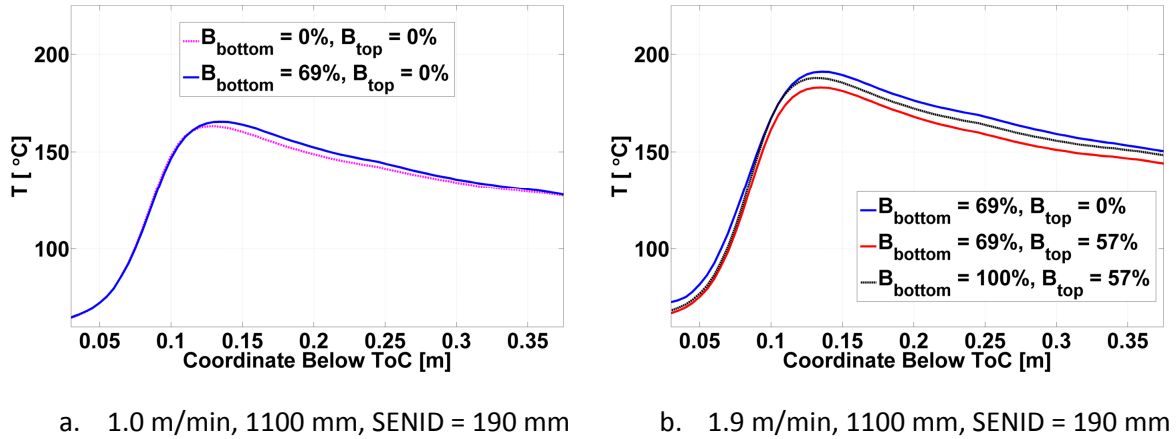
Figure 2. Average vertical temperature distribution along OptiMold Monitor fibers for varying magnetic fields.

In Figure 2, the collected temperature data from the optical fibers residing inside the active strand width has been averaged horizontally to a single average vertical curve. Data collected over 2 minutes of constant casting conditions has been averaged with respect to time, to show a single average vertical temperature distribution curve for the entire active mold per case. In Figure 2a, a lower casting speed was used and only the bottom level FC Mold magnetic field was applied. With the magnetic field positioned just below the exit ports of the SEN, there is a general containment of heat in the upper part of the mold as the magnetic field restricts downward penetrating flow.

As the casting speed is increased, the necessity for flow stability and control grows. The solidifying shell becomes thinner, and more thermal energy from the strand is cooled away in the mold, resulting in generally higher temperatures. Results in Figure 2b show a general temperature decrease in the upper part of the mold when applying the top level magnetic field of the FC Mold, here a suppression by 8 °C. As the bottom field is further strengthened, the temperature peak lifts with the same reason given for Figure 2a.

The temperature measurements at a fiber close to the center of the strand (x=25 mm) and at a fiber close to one of the mold narrow faces (x=425 mm) reveal different shaped vertical temperature curves at different positions. At constant casting conditions, the bottom and top FC Mold magnetic fields were varied to produce different molten steel flow patterns inside the mold. At high casting speed, configurations with weak top magnetic fields tend to have very pronounced temperature peaks close to the mold narrow faces compared to at the center of the mold, as shown in Figure 3. The different magnetic field strengths amount to temperature differences exceeding 20 °C at the location of the edge fibers.
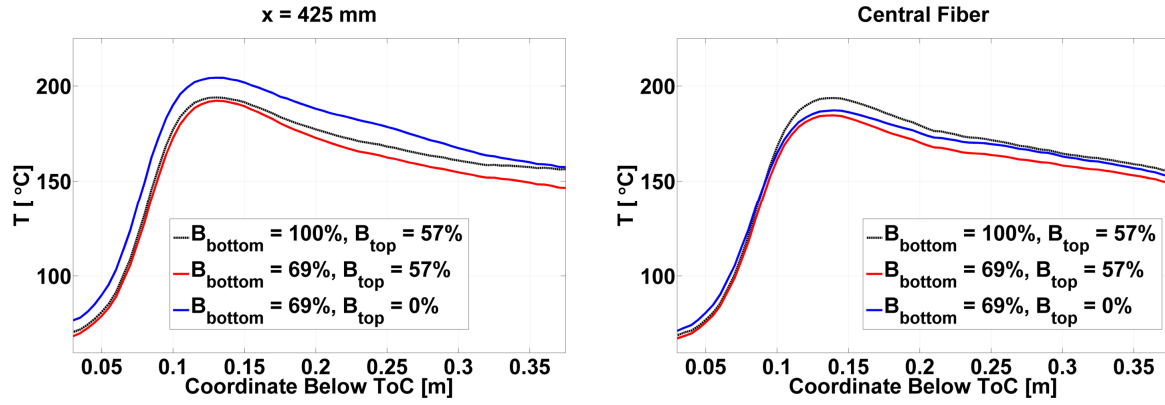
Figure 3. Time averaged vertical temperature profiles along different optical fibers for varying magnetic fields. Mold dimensions = 237x1100 mm, casting speed = 1.9 m/min, SEN immersion depth = 190 mm.

The time variation along these fibers is displayed in Figure 4 using the standard deviation. It is evident that a weaker top field corresponds to higher temperature fluctuations close to the narrow faces, whilst a more stable behavior is observed toward the center of the strand.
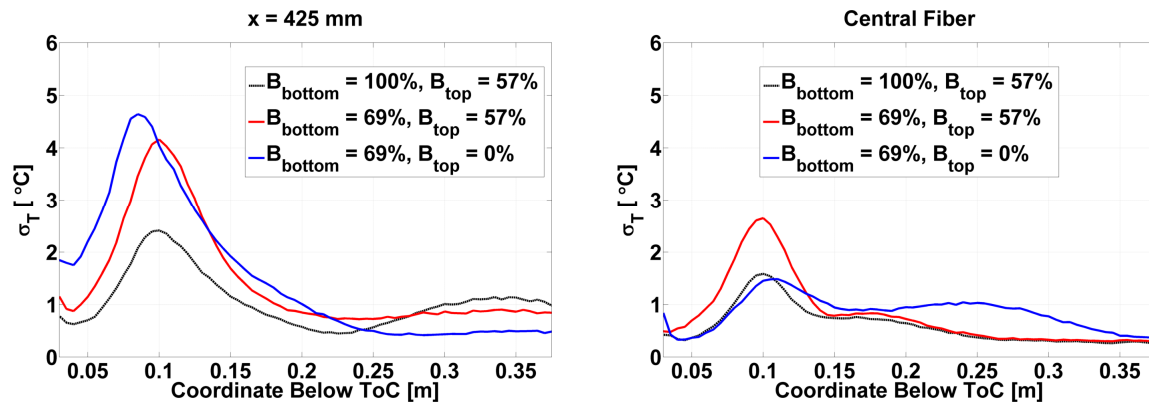

Figure 4. Distribution of vertical temperature profile standard deviation for different fibers and varying magnetic fields. Mold dimensions = 237x1100 mm, casting speed = 1.9 m/min, SEN immersion depth = 190 mm.

The observed different vertical temperature distributions can be explained by different melt flow patterns. This is further exploited in the time averaged temperature maps shown in Figure 5. A strong top magnetic field (Figure 5a) results in a relatively homogeneous temperature distribution. For a vanishing top magnetic field (Figure 5c), the temperature distribution becomes inhomogeneous with accentuated hot-spots close to the narrow faces.
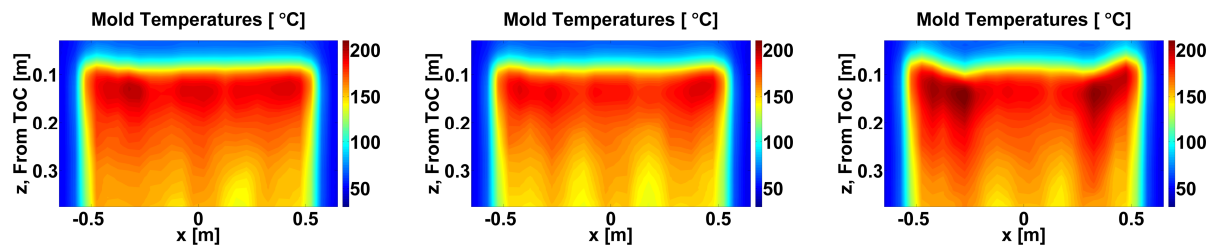

Figure 5. Time averaged OptiMold Monitor 2D heat maps for different FC Mold magnetic field configurations (B_{bottom}/B_{top}). a. 100/57%, b. 69/57%, c. 69/0%.

Based on the measured temperature distributions, the meniscus shape has been estimated (see Appendix). Figure 6 illustrates the resulting time averaged calculated meniscus shape for the FC Mold configurations described above for the 1100 mm width, 190 mm SEN immersion depth and 1.9 m/min casting speed.
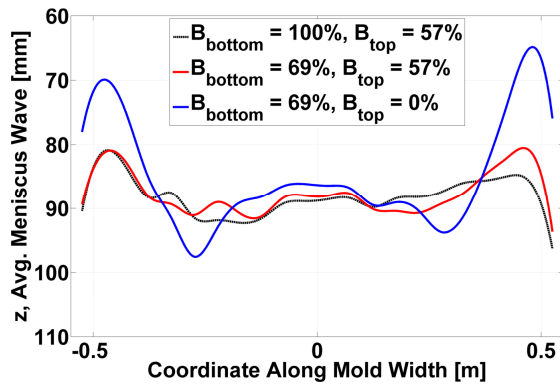

Figure 6. Meniscus shape along the width of the mold for different FC Mold settings. Estimated from measured temperature.
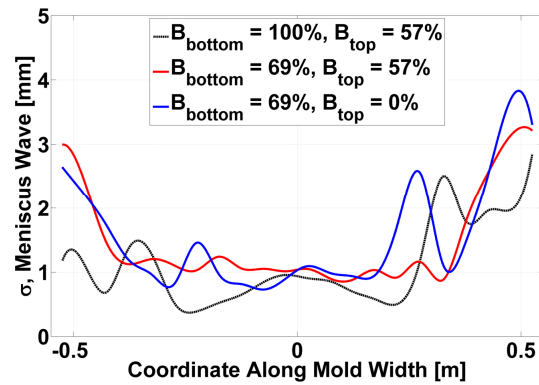
Figure 7. Standard deviation of the meniscus height over the entire mold width for different FC Mold settings.

The estimated meniscus shape results indicate that the stronger top magnetic fields ensure a lower wave peak close to the narrow faces, whereas the meniscus wave height is much more pronounced for the unbraked top domain. An estimate of the dynamic meniscus fluctuations shown in Figure 7 also indicates a stabilization over the entire width of the mold with the application of magnetic fields.
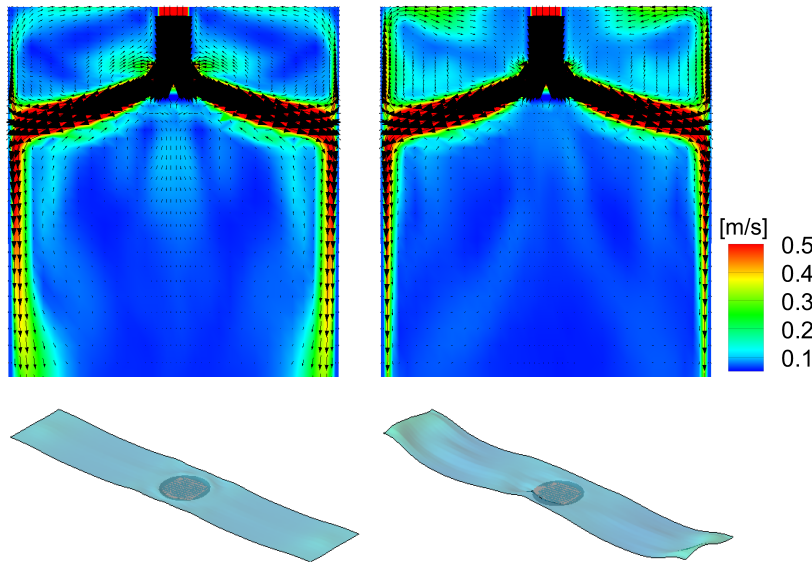

Figure 8. Simulated flow speed in center slice of strand and calculated meniscus shape for varying FC Mold magnetic fields (B_{bottom}/B_{top}). a. 100/57%, b. 69/0%.

A set of numerical simulations of the molten steel flow in the mold illustrates the causes of the observed meniscus shapes and flow speeds. Figure 8 shows the results of computer simulations of the 237x1100 mm, 1.9 m/min scenario. The top row displays the time averaged flow velocity in the center slice of the strand. In the bottom row the corresponding calculated meniscus shape is presented.

The CFD-simulated and the OptiMold Monitor estimated meniscus shapes in Figure 8 and Figure 6 have a close resemblance. As the top magnetic field is missing, the flow pattern in Figure 8b shows a strong upward directed flow along the upper part of the narrow faces. This vertical momentum pushes the meniscus wave upward and creates a high crest of potential energy close to the narrow face; energy that is converted into kinetic energy

in the form of meniscus flow speed towards the SEN. For the stronger top magnetic field in Figure 8a, the upper recirculation loop is restricted in speed and hence has a flatter meniscus with lower flow speeds. The strong bottom field in Figure 8a restricts the downward directed flow momentum, hence reducing the penetration depth of the lower recirculation loop.
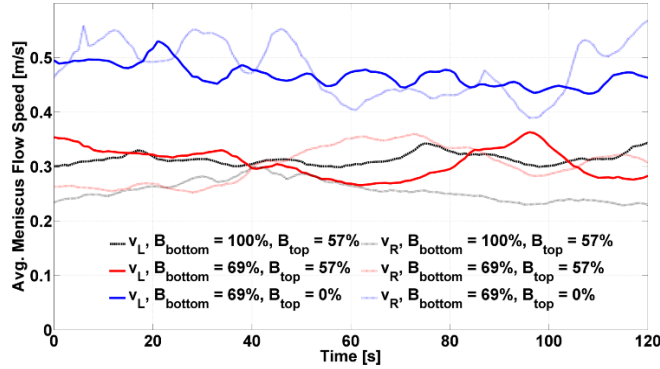

Figure 9. Calculated meniscus flow speeds, left and right hand side of mold, for different FC Mold configurations.

Based on the meniscus shape, the meniscus flow speed can be calculated. In Figure 9, the variation of the meniscus flow speed is given over the 2 min trial period. The coupling between the top magnetic field and the meniscus general flow speed level is apparent. It is also clear that the unbraked high flow speeds undergo large fluctuations as well as left/right-asymmetry over time. A stable meniscus flow level around 0.3 m/s is in this 237x1100 mm, 1.9 m/min casting sequence found for an FC Mold field setting of 57%/100% (top/bottom).

Meniscus Shape and Flow Speed Control

Figure 10 illustrates an instantaneous OptiMold Monitor thermal measurement over the broad face for a slab of width 1100 mm cast at 1.8 m/min, converted into the estimated meniscus wave profile given in Figure 11.
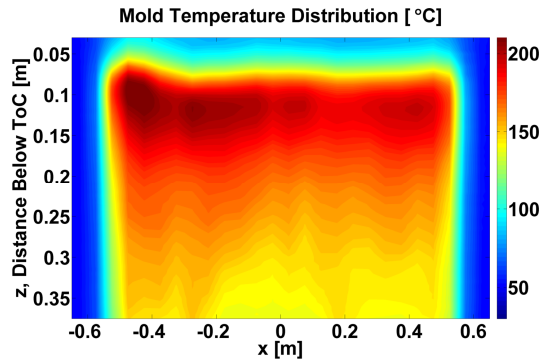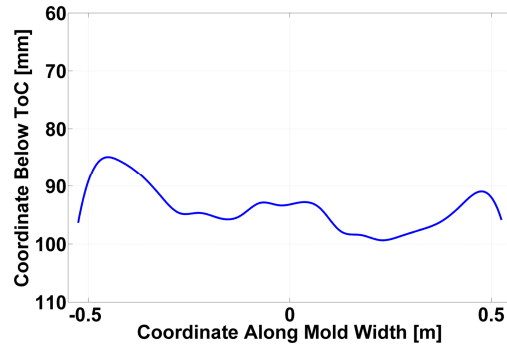

Figure 10. Measured mold temperature map.

Figure 11. Estimated meniscus shape.

At this instant in time, two nailboards with 18 nails each, one on each side of the SEN, were dipped into the meniscus registering flow speeds in the molten steel. Nailboard measurement analysis [7] gave the meniscus flow speed distribution illustrated in Figure 12, i.e. a double roll flow pattern with meniscus flows from the narrow faces toward the SEN.

Figure 12. Nailboard flow velocity results [m/s]. Casting width 1100 mm, 1.8 m/min.

Assuming a typical double roll mold flow pattern, melt flows upward along the narrow faces to the meniscus where a standing wave crest stores potential energy. The corresponding kinetic energy is released as meniscus flow velocity toward the SEN. The general measured flow speeds are 0.3-0.45 m/s, with biased flow speeds on the left hand side. This corresponds well to the higher estimated meniscus wave peak on the left given in Figure 11.

To obtain statistical reliability, and to cover a range of different casting conditions, data from a large set of nailboard tests was collected. This data establishes a connection between the estimated meniscus standing wave shape and the measured meniscus flow speed and pattern. This means that the by OptiMold Monitor measured temperature profiles, via an estimate of the meniscus wave profile, are capable of deducing meniscus flow speeds in real-time.

Implementing the algorithms for meniscus profile estimates and flow speed in the OptiMold System Analysis Unit, the deduced in-mold flow speeds can be monitored over time. In Figure 13, the meniscus wave height has been monitored over the last two heats of a casting sequence before tundish and SEN change.
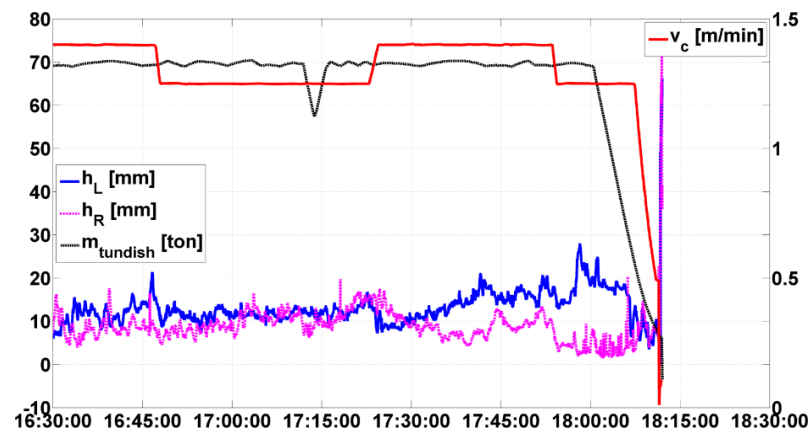

Figure 13. Monitored left and right hand side estimated meniscus wave heights (h_L and h_R) for last 2 heats before tundish and SEN change.

Before the ladle change at 17:14, the temperature distribution and meniscus wave are relatively symmetric, a snapshot at 17:10 is displayed in Figure 14(top). In the last part of the sequence, the asymmetry becomes more pronounced biasing the meniscus wave on the left side. It can be concluded that clogging affects the flow pattern symmetry in the last stages of casting.

These results reveal the potential of the OptiMold Monitor in conjunction with a flow control device to be able to counteract and control in-mold flow asymmetries immediately as they are detected by the temperature measurements. A modern generation FC Mold has the ability to control left and right side magnetic fields independently and consequently apply different electromagnetic forces to the mold flow on left and right sides, thus being a perfect fit for OptiMold Control to regulate symmetry as well as the appropriate flow speed levels in real time.
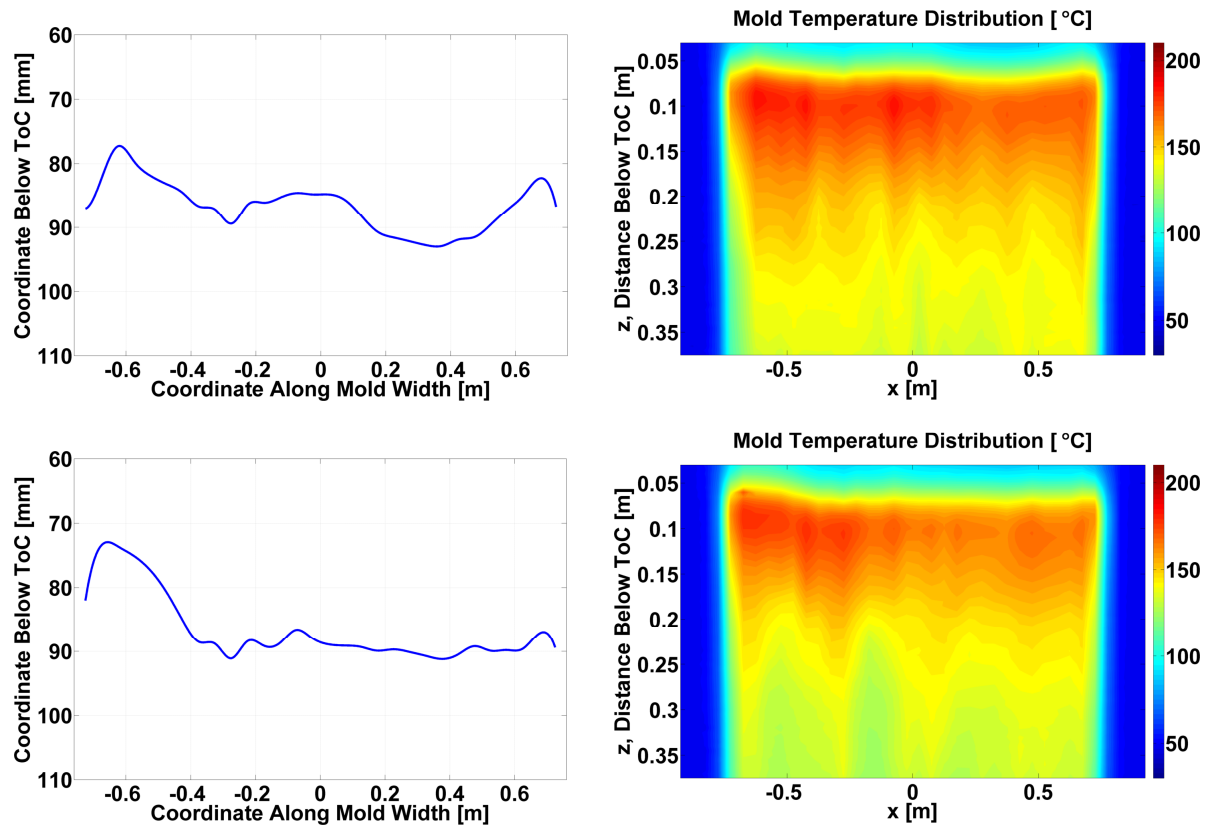
Figure 14. Estimated meniscus shape profiles and measured mold temperature distributions at instants 17:10 (top row) and 18:00 (bottom row).

Conclusions

The temperature distribution over the height of the mold is measured in high resolution by the OptiMold Monitor. This enables powerful analysis of the casting process with a highly resolved visualization of the thermal situation in the mold. The influence on thermal mold distributions and meniscus shape by various casting parameters can now be studied in detail.

The OptiMold Monitor can through high-resolution temperature measurements detect mold flow pattern characteristics such as meniscus shape, flow velocity and flow asymmetry. This opens up possibilities for enhanced mold flow control where OptiMold Monitor in a closed-loop connection to an electromagnetic actuator can damp or accelerate flow speeds as well as control flow asymmetry.

Additionally, a fiber optic mold temperature measurement system of high resolution can extend functionality and performance of conventional thermocouple systems and detect local thermal phenomena. Fiber optics measure undisturbed in the presence of magnetic fields.

References

[1] S. Kenichiro et al., "Flow field control of liquid steel in the mold of a continuous slab caster by an electromagnetic brake", Tetsu-to-Hagane (1983), Vol. 69, No.12, pp. 912

[2] H. Okuda et al., "Effects of electro-magnetic brake on surface quality of medium carbon strand cast slabs", Tetsu-to-Hagane (1986), Vol. 72, No.4, pp. 196

[3] H. Yamamura, T. Toh et al., "Optimum magnetic flux density in quality control of casts with level DC magnetic field in continuous casting mold", ISIJ International (2001), Vol.41, No. 10, pp.1229-1235

[4] Y. Miki, S. Takeuchi, "Internal defects of continuous casting slabs caused by asymmetric unbalanced steel flow in mold", ISIJ International (2003), Vol. 43, No. 10, pp. 1548-1555

[5] A. Asseh et al.,"A writing technique for long fiber Bragg gratings with complex reflectivity profiles", Lightwave Technology, Volume 15, 1997, Issue 8, pp. 1419-1423.

[6] J. Kromhout, S. Carless, E. Dekker, C. v. Kralingen, "Revealing the Unknown: Monitoring the In-Mould Performance during Continuous Casting of Steel", 8th ECCC (Graz, 2014), pages 982-993.

[7] R. Liu et al., "Measurement of molten steel surface velocity with SVC and nail dipping during continuous casting", TMS (2011), PP. 51-58

[8] J. Sengupta, B. Thomas, and M. Wells, "The Use of Water Cooling During the Continuous Casting of Steel and Aluminum Alloys," Metallurgical and Materials Transactions A – Physical Metallurgy and Materials Science, 36A:1, 187-204, Jan., 2005.

[9] JJ. Bikerman, "Physical surfaces", New York (NY): Academic Press; 1970.

[10] G. Hedin, A. Kamperman, M. Sedén, K. Fröjdh, J. Pejnefors, "Exploring Opportunities in Mold Temperature Monitoring Utilizing Fiber Bragg Gratings", To Be Presented at SCANMET V, (Luleå, 2016).

[11] L. Hibbeler et al., "Calibration of Thermal Models of Continuous Casting Molds", Iron and Steel Technology - AIST Transactions, 10:9, 199-210, Sept., 2013.

[12] M. Sedén et al., "Control of Flow Behavior by FC Mold G3 in Slab Casting Process", 8th European Continuous Casting Conference, Graz, Austria, 2014, Proceedings pp. 558-569.

[13] D. Lieftucht et al., "HD Mold – A New Fiber-Optical-Based Mold Monitoring System", Iron and Steel Technology - AIST Transactions, 10(12):87-95, Dec., 2013.

Appendix: Calculation of Meniscus Wave Shape from Mold Temperatures
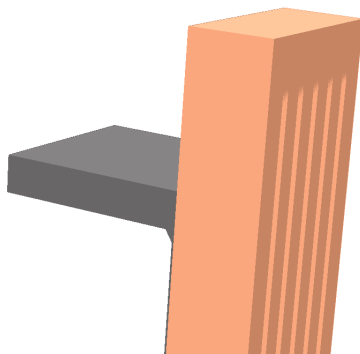

Figure 15. Simple model of slice of top of mold copper plate and mold flux.

Thermophysical conditions at the top of the mold are complex. Factors such as meniscus topology, mold flux dimensions and properties, shell solidification and oscillation marks determine the heat transfer from the steel in the strand to the mold cooling at the back end of the mold copper plates [8].

By 3D-numerical modeling of the thermal transport from the steel via the mold flux through the mold copper plate to the cooling channels, the temperature distribution in the very top part of the copper plate has been investigated with respect to meniscus shape and position.

Using a hypothetical step-shaped meniscus of height 10

mm placed 100 mm below the top of copper, a Bikerman approximation of the meniscus topology closest to the mold wall [8], and a thin mold flux layer in between the steel and the copper plate, isotherms have been calculated in the plane of the optical fibers.
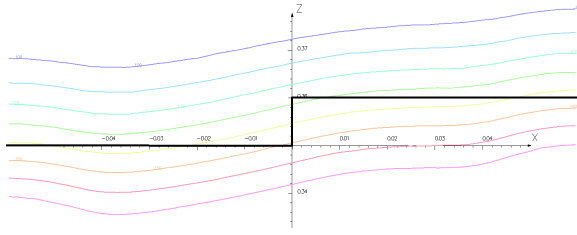

Figure 16. Numerically simulated isotherms, 100-170 °C, in Cu-mold above meniscus, in plane 15 mm from hot face. The far-field step-meniscus shown as reference in black.

The results displayed in Figure 16 show that the isotherms 15 mm from the hot face are approximately equally spaced vertically. Local dips on the isotherms are caused by the vicinity to the cooling channels. The isotherm rise from left side to right side is approximately 9 mm, i.e. very close to the actual height of the assumed step-meniscus of 10 mm. This means that the actual meniscus profile can be closely imitated, after a minor re-scaling, by a measured isotherm from the OptiMold Monitor.
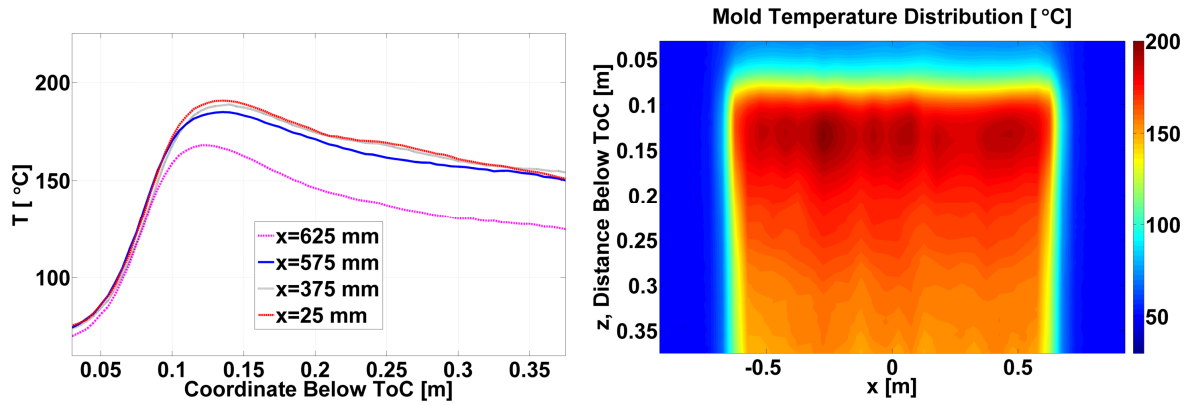

Figure 17. a. Measured vertical T-profiles at different fibers. b. Full 2d-representation of measured OptiMold Monitor temperature distribution.

The measured temperature profiles along the OptiMold System optical fibers show a linear ascent in the 10-40 mm region above the meniscus. In this wide linear temperature range, which is casting speed dependent, all isotherms capture the meniscus shape equally well. In practice, this allows the meniscus shape to be sufficiently estimated by the profile of any isotherm in the linear temperature region. With the high resolution measurements of the OptiMold Monitor, an interpolation routine creates high-quality isotherms. The vertical coordinate of the meniscus can be determined either by coupling to the eddy-current mold level sensor, or e.g. by fitting a model distribution to the actually measured vertical temperature curves 15 mm into the copper from the hot face. Hence, a good estimate of the meniscus profile across the entire mold width can be created from the heat distribution measured in the very top of the mold.